Appl Biochem Biotechnol (2014) 172:497–508
DOI 10.1007/s12010-013-0538-y

Canine Parvovirus Type 2a (CPV-2a)-Induced Apoptosis in MDCK Involves Both Extrinsic and Intrinsic Pathways

Juwar Doley · Lakshya Veer Singh · G. Ravi Kumar · Aditya Prasad Sahoo · Lovleen Saxena · Uttara Chaturvedi · Shikha Saxena · Rajiv Kumar · Prafull Kumar Singh · R. S. Rajmani · Lakshman Santra · S. K. Palia · S. Tiwari · D. R. Harish · Arvind Kumar · G. S. Desai · Smita Gupta · Shishir K. Gupta · A. K. Tiwari

Received: 4 July 2013 / Accepted: 15 September 2013 /
Published online: 4 October 2013

Abstract The canine parvovirus type 2 (CPV-2) causes an acute disease in dogs. It has been found to induce cell cycle arrest and DNA damage leading to cellular lysis. In this paper, we evaluated the apoptotic potential of the "new CPV-2a" in MDCK cells and elucidated the mechanism of the induction of apoptosis. The exposure of MDCK cells to the virus was found to trigger apoptotic response. Apoptosis was confirmed by phosphatidylserine translocation, DNA fragmentation assays, and cell cycle analysis. Activation of caspases-3, -8, -9, and -12 and decrease in mitochondrial potential in CPV-2a-infected MDCK cells suggested that the CPV-2a-induced apoptosis is caspase dependent involving extrinsic, intrinsic, and endoplasmic reticulum pathways. Increase in p53 and Bax/Bcl2 ratio was also observed in CPV-2a-infected cells.

Keywords Apoptosis · Caspase · CPV-2 · MDCK cells · Apoptotic pathways

Introduction

Apoptosis is an orchestrated, genetically regulated, and finely tuned phenomenon of cell death, which is quintessential for embryogenesis, development, and tissue homeostasis of multicellular organisms [1]. It is characterized by nuclear and cytoplasmic condensation, DNA fragmentation, plasma membrane blebbing, and apoptotic body formation [2]. Many DNA and RNA viruses including Newcastle disease (NDV), vesicular stomatitis (VSV),

J. Doley · L. V. Singh · G. R. Kumar · A. P. Sahoo · L. Saxena · U. Chaturvedi · S. Saxena · R. Kumar · P. K. Singh · R. S. Rajmani · L. Santra · S. K. Palia · S. Tiwari · D. R. Harish · A. Kumar · G. S. Desai · S. Gupta · S. K. Gupta · A. K. Tiwari (✉)
Molecular Biology Lab, Division of Veterinary Biotechnology, Indian Veterinary Research Institute, Izatnagar, Bareilly, Uttar Pradesh 243122, India
e-mail: aktiwari63@yahoo.com

vaccinia, adeno, herpes simplex (HSV), polio, autonomous parvoviruses (APV), etc., have been shown to cause apoptosis [3–7].

Parvoviruses are small (25–30 nm), non-enveloped viruses that multiply in cell nucleus and contain a linear, single-stranded DNA consisting of two large open reading frames (ORFs) and smaller or overlapping genes, encoding for two nonstructural (NS1 and NS2) and two structural (VP1 and VP2) proteins [8]. In parvovirus infection, apoptotic cell death is one of the key pathogenic mechanisms in causing damage to tissues [9, 10]. Human parvovirus B19 has been shown to induce apoptosis in vitro in different cell types, such as hematopoietic cells [11, 12] and glioblastoma cells [13]. The human and rodent parvoviruses have been shown to have oncolytic potential as they preferentially multiply and kill tumor cells [14–16].

Canine parvovirus 2 (CPV-2), a type species in the genus *Parvovirus*, family Parvoviridae, sub family Parvovirinae causes severe, fatal hemorrhagic gastroenteritis in dogs [8]. Though initial vaccination programs helped develop herd immunity in canine populations, the host-immunity pressure has contributed to the progressive emergence of CPV-2 antigenic variants. The two antigenic variants, distinguishable using monoclonal antibodies (MAbs) were termed CPV types 2a (CPV-2a) and 2b (CPV-2b). Currently, these antigenic variants have completely replaced the original type 2 [8]. CPV-2a and CPV-2b differ in five or six aa residues of the VP2 capsid protein from the original strain CPV-2. In contrast, only two residues differentiated CPV-2a from CPV-2b [8, 17]. A new genetic variant of prototype CPV-2a (new CPV-2a) with nonsynonymous substitution at the VP2 amino acid residue 297 from Ser to Ala has also been reported [8, 18].

CPV-2 was found to induce apoptosis in Norden laboratory feline kidney (NLFK) cells and canine fibroma cells (A72) [19]. However, the induction of apoptosis by "new CPV-2a" and the mechanism have not been established to date. We report that "new CPV-2a"-induced apoptosis in MDCK cells is caspase and p53 dependent.

Materials and Methods

Cells and Virus

MDCK cells obtained from National Centre for Cell Sciences (NCCS), Pune, India, were used in this study. These cells were grown and maintained in Dulbecco's Modified Eagles Medium (DMEM) supplemented with 8 % fetal calf serum (FCS) and 50 μg/ml each gentamicin and nystatin (Invitrogen, USA). Canine parvovirus-2 isolated from a 2009 outbreak in Faizabad, UP, India was characterized to be "new CPV-2a." Briefly, a 1,296 bp fragment of VP2 gene was amplified, sequenced, and analyzed [8]. The sequence was submitted to GenBank with accession no. KC713932. The virus adapted to grow in MDCK cells at passage level 5 having titre of $10^{5.8}$ $TCID_{50}$ per millilitre was used in this study.

Infection of MDCK Cells

The MDCK cells grown to 30–40 % confluency were infected with 0.1 m.o.i. of MDCK adapted CPV-2a. The infected cells were harvested at 24, 48, and 72 h postinfection (p.i.) to carry out the study. The uninfected MDCK cells acted as mock control.

Assessment of Cell Viability

Cell viability assay was performed by trypan blue dye exclusion test. Briefly, both healthy and CPV-2a infected cells harvested at 24, 48, and 72 h p.i. were mixed with equal volume

of 0.2 % trypan blue solution and live unstained cells were counted using Countess cell counter (Invitrogen, USA).

Study of Apoptosis

DNA Fragmentation Assays

DNA fragmentation is one of the hallmarks in cells undergoing apoptosis [20] which was detected by gel electrophoresis, Hoechst staining, and terminal deoxynucleotidyl transferase TdT-mediated dUTP nick end labeling (TUNEL) assay.

1. *Agarose gel electrophoresis*: CPV-2a-infected and -uninfected healthy cells were harvested at 24, 48, and 72 h p.i., and DNA was isolated and analyzed by electrophoresis on 1.5 % agarose gel as described by [21].
2. *Hoechst staining*: MDCK cells grown to 30–40 % confluency were infected with CPV-2a. After 48 h p.i., cells were processed for Hoechst staining. Media from culture flasks were aspirated carefully and cells were washed once with phosphate buffer solution (PBS) and fixed with 3 % PFA for 20 min at RT. Fixing solution was aspirated, and ice-cold absolute methanol was added for 15 min to permeabilize the cells. Cells were washed thrice with PBS and incubated with Hoechst 33258 (0.12 μg/ml, final concentration in PBS) solutions for 15 min at RT. Cells were visualized with Nikon fluorescence microscopy under ×40 objective [9].
3. *TUNEL Assay*: The DNA fragmentation (internucleosomal cleavage) in CPV-2a-infected cells was also examined by APO-BrdU TUNEL Assay Kit (Invitrogen) as described by the manufacturer. Briefly, 2×10^6 cells were fixed with 5 ml of 1 % (*w*/*v*) paraformaldehyde for 15 min on ice. After washing, the fixed cells were resuspended in 0.5 ml of PBS and 5 ml of ice-cold 70 % (*v*/*v*) ethanol and incubated at −20 °C for 18 h. The cell pellet obtained after centrifugation was resuspended in 50 μl of the DNA labeling solution (10 μl of reaction buffer, 0.75 μl of TdT enzyme, 8.0 μl of BrdUTP, and 31.25 μl of dH_2O) for 60 min at 37 °C in a waterbath. After washing the cells with rinse buffer, cell pellet was incubated with 100 μl of the diluted antibody solution for 30 min at room temperature in dark. Stained cells were analyzed in a flow cytometer using FL1 filter.
4. *Detection of hypodiploid cells population by flow cytometry and cell cycle analysis*: The increase in number of hypodiploid cells during apoptosis can be detected by staining with propidium iodide (PI). Therefore, to quantitate number of hypodiploid cells, both mock-infected and CPV-2a-infected cells were harvested at different time intervals and stained with PI for 15 min at 37 °C as described previously [21] and analyzed by flow cytometry.

Phosphatidylserine Translocation by Annexin V-Binding Assay

Phosphatidylserine (PS) translocation to outer leaflet of plasma membrane reveals information about cells undergoing apoptosis. This PS translocation was detected using Vybrant Apoptosis Assay Kit (Invitrogen, USA). Briefly, 1×10^6 cells/ml were harvested by trypsinization at 24, 48, and 72 h p.i. and resuspended in 100 μl 1X annexin-binding buffer. To this, 5 μl of Alexa Fluor® 488 annexin V and 1 μl of the 100 μg/ml PI solution were added and incubated at room temperature for 15 min. Subsequently, 400 μl of 1X annexin-

binding buffer was added, and cells were kept on ice and analyzed by flow cytometry using FL1 and FL3 bandpass filters (FACS Calibur, Becton Dickinson, USA).

Elucidation of Pathways

Detection of Loss of Mitochondrial Membrane Potential ($\Delta\psi m$) by Flow Cytometry

Alteration in mitochondrial membrane potential caused by "new CPV-2a" infection to MDCK cells was detected using 5,5′,6,6′-tetrachloro-1,1′,3,3′-tetraethylbenzimidazol carbocyanine (Mitoprobe™ JC-1 assay kit, Invitrogen, USA) by flow cytometry following the instructions of the manufacturer. Briefly, 10^6 MDCK cells, grown in six-well plates were infected with CPV-2a. The cells were harvested by trypsinization at 24 and 48 h p.i. and resuspended in 1 ml warm medium. The cells were stained with JC-1 dye (5,5′,6,6′-tetrachloro-1,1′,3,3′-tetraethyl benzimidazolyl carbocyanine iodide) following the manufacturer's protocol and analyzed on a flow cytometer with 488 nm excitation using FL1 and FL2 filters. A red to green shift in fluorescence indicates the decrease in mitochondrial membrane potential.

Detection of p53 Activation by Flow Cytometry

Activation of p53 was examined by flow cytometry using rabbit monoclonal p53 antibody (BD Biosciences). Briefly, infected and control cells were harvested at 24, 48, and 72 h p.i., and fixed with 3 % paraformaldehyde for 20 min at RT. After washing twice with ice-cold PBS, the cells were incubated with rabbit monoclonal p53 antibody (BD Biosciences) for 1 h at 37 °C and analyzed in flow cytometer using FL1 filter (Becton Dickinson).

Detection of Caspase-3 and Caspase-8 Activation by Flow Cytometry

Activation of caspase-8, the initiator caspase in extrinsic pathway, and caspase-3, the main effector caspase in cells undergoing caspase dependent apoptosis, was detected using Vybrant ® FAM caspase-8 assay Kit and Vybrant ® FAM caspase-3 assay Kit (Invitrogen, USA), respectively. The assay was performed as per manufacturer's protocol. Briefly, 2×10^5 cells suspended in culture media was incubated with10 μl of 30X FLICA working solution for 60 min at 37 °C in a CO_2 incubator protected from light. After incubation, cells were washed twice with 1X wash buffer and resuspended in 400 μl of 1X wash buffer and analyzed in flow cytometer using FL1 filter.

Expression of Caspases-3, -8, -9, and -12, p53, Bax, and Bcl2 by Real-Time PCR

The total RNA isolated from cells infected with CPV-2a at all times points was reverse transcribed to cDNA, using QuantiTect Reverse Transcription Kit (QIAGEN, Germany), according to the manufacturer's instruction. The sequences of the primers used in the study are given in Table 1. A melting curve analysis was performed to know the specificity of qPCR. For the test gene and endogenous control standards, tenfold serial dilutions were run in the study to estimate the efficiency of PCR, and the percentage efficiency ranged between 90 and 100 %. All the samples were run in triplicates. The relative expression of each sample was calculated using the $2^{-\Delta\Delta CT}$ method [21–23]. Results were analyzed and shown as fold change ($2^{-\Delta\Delta CT}$) relative to the control group.

Table 1 Primers used for quantitative real-time PCR

Gene	Real-time PCR primers (5′–3′)	Product length (bp)
Caspase 3	Forward : TTCATTATTCAGGCCTGCCGAGG	83
	Reverse : TTCTGACAGGCCATGTCATCCTCA	
Caspase 8	Forward: ACAAGGGCATCATCTATGGCTCTGA	70
	Reverse : CCAGTGAAGTAAGAGGTCAGCTCAT	
Caspase 9	Forward: TCAGTGACGTCTGTGTTCAGGAGA	97
	Reverse : TTGTTGATGATGAGGCAGTAGCCG	
Caspase 12	Forward : GCCGTCTGGGTGACTGATG	70
	Reverse : CTGCAAGGGCTGGTCACAT	
p53	Forward: TAACAGTTCCTGCATGGGCGGC	166
	Reverse: AGGACAGGC ACAAACACGCACC	
Bax	Forward: TTCCGAGTGGCAGCTGAGATGTTT	79
	Reverse : TGCTGGCAAAGTAGAAGAGGGCAA	
Bcl_2	Forward: CATGCCAAGAGGGAAACACCAGAA	76
	Reverse : GTGCTTTGCATTCTTGGATGAGGG	
HPRT	Forward: AGCTTGCTGGTGAAAAGGAC	104
	Reverse : TTATAGTCAAGGGCATATCC	

HPRT hypoxanthine phosphoribosyl transferase (endogenous control)

Statistical Analysis

All the experiments were run in triplicates. The results of three independent were reported as mean + SE. As the normality test failed, the Mann–Whitney nonparametric test was done in JMP 9 (SAS Institute Inc., Cary, NC, USA). Differences between groups within time were considered significant at $P \leq 0.05$.

Results

CPV-2a Induces Cytotoxicity in MDCK Cells

MDCK cells were infected with 0.1 m.o.i. of CPV-2a, and viable cells were counted in Countess cell counter to assess the cytotoxic effect of the virus. At 24 h p.i., no marked difference in viable cell population between mock control and CPV-2a infected cells was observed, whereas at 48 and 72 h p. i., decrease in viable cell percentage was observed in CPV-2a-infected MDCK cells (Fig. 1a).

CPV-2a-Induced Cytopathic Changes in MDCK Cells are Due to Apoptosis

CPV-2a Induces Internucleosomal Cleavage

To determine if the cytopathic changes in CPV-2a-infected MDCK cells were due to the induction of apoptosis, the cellular DNA from infected cells was analyzed in 1.5 % agarose gel. Presence of DNA ladder at 48 h p.i. and absence at 24 h p.i suggested fragmentation of DNA and induction of apoptosis in MDCK cells after 24 h of infection (Fig. 1b). No

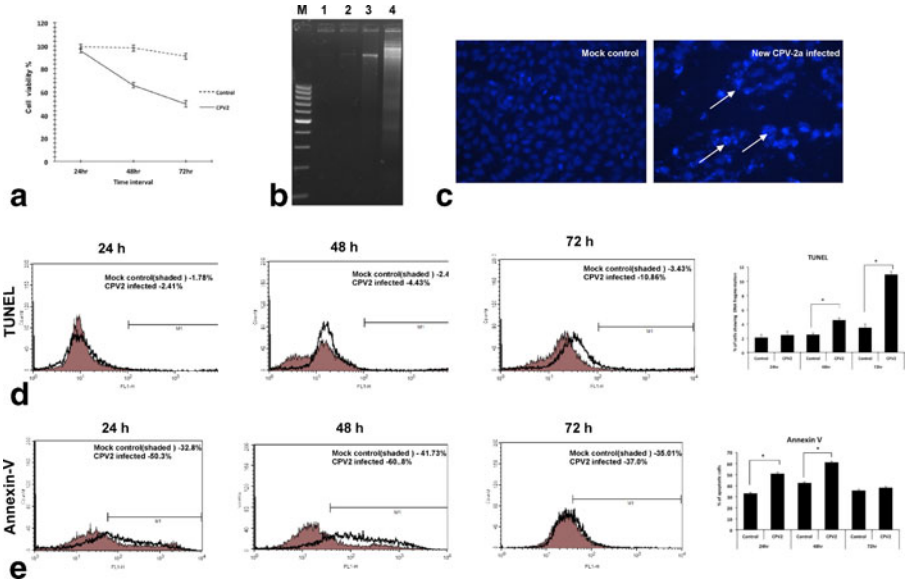

Fig. 1 **a** Cell viability was determined by trypan blue dye exclusion assay using an automated cell counter at 12, 24, and 72 h p.i. Mean (three independent observations) values of viability percentages were plotted at different time intervals. **b** DNA fragmentation in the "new CPV-2a"-infected cells. *Lane M* 100 bp DNA marker (MBI, Fermentas), *Lane 1* DNA from mock-infected cells 24 h p.i., *Lane 2* DNA from CPV-2a-infected MDCK cells 24 h p.i., *Lane 3* DNA from mock-infected cells 48 h p.i., and *Lane 4* DNA from CPV-2a-infected MDCK cells 48 h p.i. Prominent DNA ladder pattern was obtained at 48 h p.i., indicating induction of apoptosis in CPV-2a-infected MDCK cells. **c** Hoechst staining of mock-infected cells 48 h p.i. No condensation of chromatin/fragmented nuclei was observed in mock-infected cells and CPV-2a-infected cells 48 h p.i., showing condensation of chromatin/fragmented nuclei. **d** Percentage of TUNEL-positive cells in mock- and "new CPV-2a"-infected cells at 24, 48, and 72 h p.i. Percentage of TUNEL-positive cells increased significantly in CPV-2a-infected cells at 48 and 72 h p.i., indicating apoptosis. **e** Percentage of annexin V-positive cells in mock- and "new CPV-2a"-infected MDCK cells at 24, 48, and 72 h p.i. Annexin V staining detects phosphatidylserine translocation to the outer layer of plasma membrane, indicating apoptosis. The percentage of annexin V-positive cells increased significantly from mock-infected to CPV-2a-infected cells at 24 and 48 h p.i

characteristic DNA ladder pattern was seen in mock control cells. The MDCK cells infected with CPV-2a also exhibited highly condensed chromatin/fragmented nuclei upon staining with Hoechst 33342, 48 h p.i. (Fig. 1c). This DNA fragmentation was further confirmed by TUNEL assay. At 48 h p.i., 4.57±0.28 % cells were TUNEL positive as compared to 2.48±0.25 % in mock control, and the number of apoptotic cells significantly ($P \leq 0.05$) increased to 10.93±0.39 % as against 3.49±0.50 % in mock control at 72 h p.i. (Fig. 1d).

CPV-2a Infection Resulted in Translocation of Phosphatidylserine to Outer Leaflet of Plasma Membrane

Phosphatidylserine, which moves to outer leaflet of plasma membrane in the cells undergoing apoptosis, was examined by flow cytometry after staining with annexin V. The percentage of annexin V-positive cells was significantly higher at 24 h p.i. (50.75±0.98 %) and 48 h p.i. (61.01±0.84 %) than at 72 h p.i. (37.99±1.12 %) in CPV-2a-infected cells as against 32.90±0.878, 42.36±0.95, and 35.51±1.01 % in uninfected healthy MDCK cells at 24, 48, and 72 h, respectively (Fig. 1e).

CPV-2a Causes Increase in Hypodiploid Cell Count

To study the presence of hypodiploid cells (as indicated by sub-G1 peaks/M5) in CPV-2a infection, MDCK cells were examined by flow cytometry after PI staining at indicated times postinfection (Fig. 2). In CPV-2a-infected group, number of hypodiploid cell population significantly increased to 11.98±0.195 % cells at 48 h p.i. as against 6.00±0.635 % cells in mock control cells. This difference further significantly increased to 25.59±0.33 at 72 h p.i. (Fig. 2a, b).

CPV-2a-Induced Apoptosis Involves Extrinsic, Intrinsic, and Endoplasmic Reticulum Pathways

The activity of caspase-8, the initiator caspase of extrinsic pathway, significantly increased at all time points in CPV-2a-infected cells in comparison to mock control. The activity of caspase-8 was found in 3.57±0.30, 26.57±1.35, and 95.6±1.26 % cells in CPV-2a-infected MDCK group as against 2.41±0.20, 14.63±1.32, and 42.96±1.15 % cells in mock control at 24, 48, and 72 h p.i., respectively (Fig. 3a). On real-time PCR, the expression of caspase-8 was found to be upregulated by 1.09±0.34, 1.67±0.58, and 4.9±0.59 folds in CPV-2-infected cells as compared to mock control cells at 24, 48, and 72 h p.i., respectively (Fig. 3b).

A significant loss in mitochondrial transmembrane potential at all time points in CPV-2a-infected MDCK cells as compared to the mock control cells was noticed on flow cytometry (Fig. 3c). The significant increase in red to green shift is indicative of the increase in the percentage of apoptotic cells. At 24 h p.i., 20.64±0.60 % CPV-2a-infected cells showed disrupted mitochondrial membrane potential ($\Delta\psi m$) as compared to 17.62±0.42 % in mock control. This increased further to 27.77±0.51 and 47.19±0.48 % at 48 and 72 h p.i. in comparison to 20.68±0.57 and 30.91±0.45 in mock control cells, respectively. A significant increase in Bax to Bcl2 ratio at all time points was also observed in CPV-2a-infected MDCK cells (Fig. 3d). In addition, the increased expression of caspase-9 by 1.22±0.63, 2.65±0.60, and 3.89±0.59 folds in CPV-2-infected cells as compared to mock control cells at 24, 48, and 72 h p.i., respectively, indicated the involvement of intrinsic pathway real-time PCR. Caspase-12, the initiator of endoplasmic reticulum pathway, was also upregulated by 1.189±0.83, 3.10±0.27, 4.46±0.36 folds, respectively, in CPV-2-infected cells as compared to mock control cells at 24, 48, and 72 h p.i., respectively (Fig. 3f).

The activity of caspase-3, which is main executioner caspase, was determined by flow cytometry and real-time PCR. At 48 h p.i., the caspase-3 activity significantly increased in CPV-2a-infected cells (55.97±0.73 %) as compared to mock control cells (8.76±0.78 %). The activity further increased at 72 h p.i. to 85.95±0.70 % in CPV-2a-infected cells as compared to 9.63±0.28 % in mock control (Fig. 3g). The expression of caspase-3 was also found to be upregulated by 1.73±0.34, 2.36±0.58, and 9.8±0.85 folds in CPV-2-infected cells as compared to mock control cells at 24, 48, and 72 h p.i., respectively, by real-time PCR (Fig. 3h).

CPV-2a-Induced Apoptosis is p53 Dependent

Expression of p53 gene was assessed by fluorescent microscopy. Our results indicated that there was an increase in p53 activity at 48 h p.i. as compared to mock control cells, suggesting the involvement of p53 in CPV-induced apoptosis. On real-time PCR analysis, the expression of p53 was also found to be upregulated by 1.76±0.83 at 24 h, 3.33±0.54 at

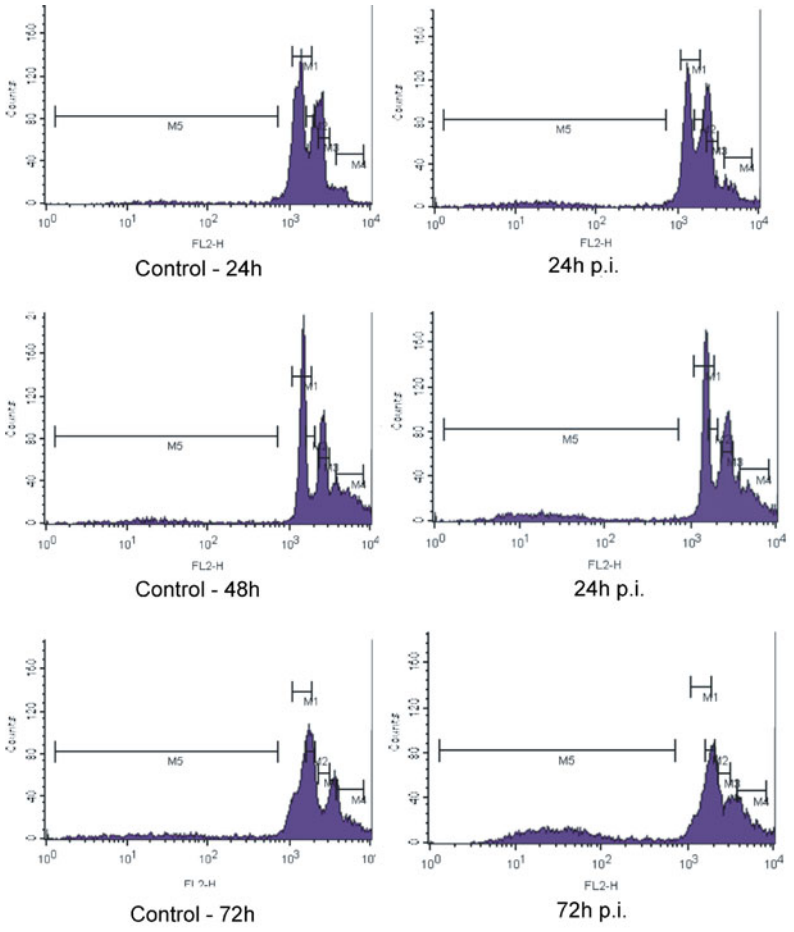

a

Phases	Control 24h	24 h p.i.	Control 48h	48 h p.i.	Control 72h	72h p.i.
M1 - G_1/G_0	47.57	43	36.89	35.40	40.64	27.93
M2 - S	20.13	20.59	7.34	9.33	18.42	20.36
M3 - G_2/M	13.12	13.83	21.36	22.68	11.59	11.47
M4 > G_2/M	3.75	6.92	18.36	14.02	10.66	12.36
M5 - Sub G1	4.11	8.09	5.78	11.74	11	25.32

b

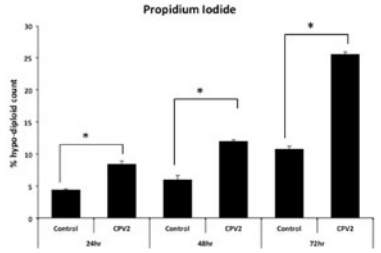

Fig. 2 **a** DNA fluorescence of "new CPV-2a"-infected cells at 24, 48, and 72 h p.i. after PI staining. Mock-infected cells revealed a typical diploid peak that gradually decreased with concomitant increase in hypodiploid peak (marked as *M5*) in CPV-infected cells. **b** Percentage of hypodiploid cells detected on PI staining in mock- and "new CPV-2a"-infected cells at 24, 48, and 72 h p.i. Hypodiploid cells significantly increased from mock-infected to CPV-infected cells at all time points

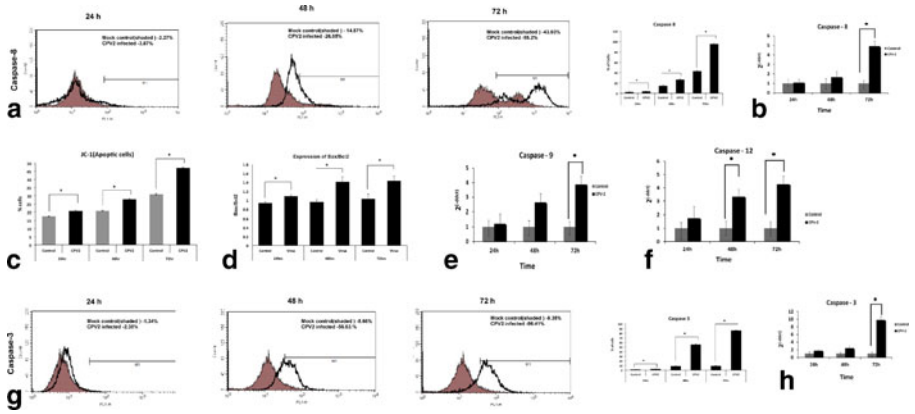

Fig. 3 **a** Percentage of cells showing caspase-8 expression in mock- and "new CPV-2a"-infected cells at 24, 48, and 72 h p.i. Caspase-8 expression significantly increased in CPV-infected cells at 72 h p.i., indicating the role of caspase-8 in CPV-2a-induced apoptosis. **b** mRNA expression levels of caspase-8 in mock and "new CPV-2a" at 24, 48, and 72 h p.i. Increase in expression indicated involvement of caspase-8. **c** mRNA expression levels of Bax and Bcl-2 shown as Bax/Bcl2 ratio in mock- and virus-infected cells at 24, 48, and 72 h p.i. Increase in Bax/Bcl-2 ratio indicated apoptosis **d** Percentage of apoptotic cells as determined by JC-1 dye indicating the loss of mitochondrial potential, in mock- and "new CPV-2a"-infected cells at 24, 48, and 72 h p.i. Apoptotic cells significantly increased in CPV-2a-infected cells at all time points. **e** mRNA expression levels of caspase-9 in mock and "new CPV-2a" at 24, 48, and 72 h p.i. Increase in expression indicated involvement of caspase-9. **f** mRNA expression levels of caspase-12 in mock and "new CPV-2a" at 24, 48, and 72 h p.i. Increase in expression indicated involvement of caspase-12. **g** Percentage of cells showing caspase-3 expression in mock- and "new CPV-2a"-infected cells at 24, 48, and 72 h p.i. Caspase-3 expression significantly increased in CPV-infected cells at 72 h p.i., indicating the role of caspase3. **h** mRNA expression levels of caspase-3 in mock and "new CPV-2a" at 24, 48, and 72 h p.i. Increase in expression indicated involvement of caspase-3

48 h, and 4.26±0.62 folds in CPV-2-infected cells as compared to mock control cells post at 24, 48, and 72 h p.i., respectively (Fig. 4a, b).

Discussion

Apoptosis or programmed cell death is a physiological process required for maintaining cell homeostasis [24] and also one of the main mechanisms of viral pathogenesis. Parvoviruses (B19 and minute virus of mouse, H1 parvovirus), have inherent property to induce apoptosis [14]. It has been established that H1 parvovirus of human and minute virus of mouse have preferential oncolytic property in vitro in SV40 transformed cells [15, 25]. The present study was undertaken to explore the apoptotic potential of "new CPV-2a" in MDCK cells and elucidate the mechanism involved in induction of apoptosis.

Apoptosis is distinguished from necrosis by characteristic morphological and biochemical changes including compaction and fragmentation of nuclear chromatin, shrinkage of the cytoplasm, and loss of membrane asymmetry. The apoptotic ability of the "new CPV-2a" was established by various parameters including DNA fragmentation, Hoechst staining, TUNEL assay, and phosphatidylserine translocation [3, 21, 22, 26, 27]. The activation of caspases-3, -8, -12, and -9 and p53 and change in Bax/Bcl_2 ratio were evaluated in CPV-2-infected MDCK cells to elucidate the pathway(s) involved in apoptosis.

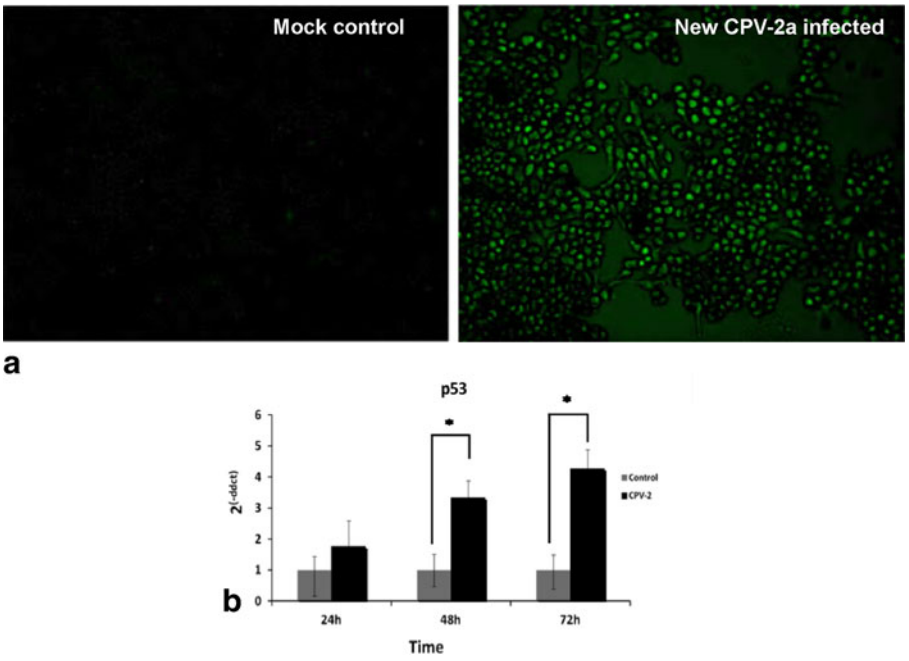

Fig. 4 **a** Photomicrograph of mock- and "new CPV-2a"-infected cells at 48 h p.i. probed with anti-p53 antibody (BD Biosciences, 1:50 dilution). **b** mRNA expression levels of p53 in mock- and virus-infected cells at 24, 48, and 72 h p.i. Increase in their expression indicated involvement of p53 in induction of apoptosis

In the cells undergoing apoptosis, activated cellular nucleases eventually digest cellular DNA into fragments consisting of multimers of approximately 200 base pairs which can be detected qualitatively by agarose gel electrophoresis and Hoechst staining and quantitatively by TUNEL assay and propidium iodide staining [12, 16, 28]. The characteristic of DNA ladder pattern noticed on agarose gel electrophoresis and the presence of fragmented nuclei upon Hoechst 33342 staining, at 48 h p.i. in the present study, indicated DNA fragmentation. This DNA fragmentation was further evaluated by TUNEL assay which relies on the presence of nicks in the DNA that are identified by terminal deoxynucleotidyl transferase enzyme that catalyzes the addition of dUTPs that are secondarily labeled with a marker. The increase in TUNEL-positive cells indicated DNA nicking and fragmentation in CPV-2a-infected cells. The significant difference in TUNEL-positive cells between the CPV-2a-infected cells and mock control cells at all time intervals suggested apoptosis. The apoptotic cells with degraded DNA appear as cells with hypodiploid DNA content and are represented in so-called "sub-G1" peaks on DNA histograms after propidium iodide staining [12, 28]. The significant increase in hypodiploid cell population, i.e., sub-G1 population, on CPV-2a infection confirmed the induction of apoptosis by the virus. Phosphatidylserine (PS), present normally on inner leaflet of plasma membrane, translocates to outer surface under apoptosis and can be detected by staining with annexin V. In CPV-2a-infected MDCK cells, the PS translocation was observed at 24 h p.i., which increased further at 48 h p.i., suggesting it an early stage event in apoptosis. Similar findings were also reported by many workers after evaluating apoptosis in different experimental models [16, 22, 23, 29].

To determine the involvement of extrinsic, intrinsic, and ER pathways, the activation of initiator caspases: caspase-8, caspase-9, and caspase-12, respectively, were evaluated at all

time points in CPV-2-infected MDCK cells. The activation/upregulation of caspase-8, caspase-9, and caspase-12 at all time points indicated the involvement of extrinsic, intrinsic, and ER pathways. The decrease in mitochondrial membrane potential and upregulation of Bax/Bcl_2 ratio confirmed the involvement of mitochondrial pathway. Further, the activation of the caspase-3, the effector caspase, confirmed that the apoptosis induced by CPV-2a is caspase dependent. Many other viruses have been reported to cause caspase-dependent apoptosis [13, 16, 25, 30, 31].

In normal healthy cells, p53 level is maintained at very low concentrations. Under certain conditions like damaged DNA, hypoxia, viral infection, etc., p53 gets activated leading to p21-mediated cell cycle arrest or apoptosis [16, 32]. The activation/upregulation of p53 in CPV-2a-infected MDCK cells at 48 h p.i. indicated the involvement of p53-mediated apoptotic pathway. Our results along with other reports suggest that the p53-mediated apoptosis may be through the up- and downregulation of Bax and Bcl_2 genes, respectively [31–33]. This study establishes that "new CPV-2a" like human and mouse parvoviruses causes apoptosis, which is p53 and caspase dependent.

Acknowledgments The authors wish to thank the Director of Indian Veterinary Research Institute, Izatnagar for providing facilities. This work was carried out by a funding from NAIP under project code C4/C3001.

References

1. Giorgi, C., Wieckowski, M. R., Pandolfi, P. P., & Pinton, P. (2011). *Communicative & Integrative Biology, 4*, 334–335.
2. Kerr, J. F., Wyllie, A. H., & Currie, A. R. (1972). *British Journal of Cancer, 26*, 239–257.
3. Everett, H., & McFadden, G. (1999). *Trends in Microbiology, 7*, 160–165.
4. Everts, B., & van der Poel, H. G. (2005). *Cancer Gene Therapy, 12*, 141–161.
5. Ravindra, P. V., Tiwari, A. K., Ratta, B., Bais, M. V., Chaturvedi, U., Palia, S. K., et al. (2009). *Virus Research, 144*, 350–354.
6. Chen, A. Y., & Qiu, J. (2010). *Future Virology, 5*, 731–743.
7. Singh, P. K., Doley, J., Kumar, G. R., Sahoo, A. P., & Tiwari, A. K. (2012). *Indian Journal of Medical Research, 136*, 571–584.
8. Decaro, N., & Buonavoglia, C. (2012). *Veterinary Microbiology, 155*, 1–12.
9. Blau, H. M., Chiu, C. P., & Webster, C. (1983). *Cell, 32*, 1171–1180.
10. Bauder, B., Suchy, A., Gabler, C., & Weissenbock, H. (2000). *Journal of Veterinary Medicine B, Infectious Diseases and Veterinary Public Health, 47*, 775–784.
11. Morita, E., Nakashima, A., Asao, H., Sato, H., & Sugamura, K. (2003). *Journal of Virology, 77*, 2915–2921.
12. Ozawa, K., Ayub, J., Kajigaya, S., Shimada, T., & Young, N. (1988). *Journal of Virology, 62*, 2884–2889.
13. Mincberg, M., Gopas, J., & Tal, J. (2011). *Virology, 412*, 233–243.
14. Angelova, A. L., Aprahamian, M., Grekova, S. P., Hajri, A., Leuchs, B., Giese, N. A., et al. (2009). *Clinical Cancer Research, 15*, 511–519.
15. Chen, Y. Q., de Foresta, F., Hertoghs, J., Avalosse, B. L., Cornelis, J. J., & Rommelaere, J. (1986). *Cancer Research, 46*, 3574–3579.
16. Ravindra, P. V., Tiwari, A. K., Ratta, B., Chaturvedi, U., Palia, S. K., & Chauhan, R. S. (2009). *Virus Research, 141*, 13–20.
17. Truyen, U. (2006). *Veterinary Microbiology, 117*, 9–13.
18. Mohan Raj, J., Mukhopadhyay, H. K., Thanislass, J., Antony, P. X., & Pillai, R. M. (2010). *Infection Genetics and Evolution, 10*, 1237–1241.
19. Nykky, J., Tuusa, J. E., Kirjavainen, S., Vuento, M., & Gilbert, L. (2010). *International Journal of Nanomedicine, 5*, 417–428.
20. Schwartzman, R. A., & Cidlowski, J. A. (1993). *Endocrine Reviews, 14*, 133–151.

21. Saxena, L., Kumar, G. R., Saxena, S., Chaturvedi, U., Sahoo, A. P., Singh, L. V., et al. (2013). *Virus Research, 173*, 426–430.
22. Schmittgen, T. D., & Livak, K. J. (2008). *Nature Protocols, 3*, 1101–1108.
23. Kumar, R., Tiwari, A. K., Chaturvedi, U., Kumar, G. R., Sahoo, A. P., Rajmani, R. S., et al. (2012). *Applied Biochemistry and Biotechnology, 167*, 2005–2022.
24. Ellis, R. E., Jacobson, D. M., & Horvitz, H. R. (1991). *Genetics, 129*, 79–94.
25. Nicoletti, I., Migliorati, G., Pagliacci, M. C., Grignani, F., & Riccardi, C. (1991). *Journal of Immunological Methods, 139*, 271–279.
26. Ohshima, T., Iwama, M., Ueno, Y., Sugiyama, F., Nakajima, T., Fukamizu, A., et al. (1998). *Journal of General Virology, 79*(Pt 12), 3067–3071.
27. Rayet, B., Lopez-Guerrero, J. A., Rommelaere, J., & Dinsart, C. (1998). *Journal of Virology, 72*, 8893–8903.
28. Yu, J., Zhang, L., Hwang, P. M., Kinzler, K. W., & Vogelstein, B. (2001). *Molecular Cell, 7*, 673–682.
29. Hay, S., & Kannourakis, G. (2002). *Journal of General Virology, 83*, 1547–1564.
30. Strasser, A., O'Connor, L., & Dixit, V. M. (2000). *Annual Review of Biochemistry, 69*, 217–245.
31. Zhang, H., Gogada, R., Yadav, N., Lella, R. K., Badeaux, M., Ayres, M., et al. (2011). *PLoS One, 6*, e16379.
32. Mousset, S., & Rommelaere, J. (1982). *Nature, 300*, 537–539.
33. Attardi, L. D., Lowe, S. W., Brugarolas, J., & Jacks, T. (1996). *The EMBO Journal, 15*, 3693–3701.